

# Influence of Excessive Moisture in the Subgrade on the Durability and Load-Bearing Capacity of Road Pavements

Mieczkowski P., Budziński B.

West Pomeranian University of Technology Szczecin

E-mail: pawel.mieczkowski@zut.edu.pl

**Abstract.** When well performed, pavement renewal or alteration shall ensure the desired properties of the road during the assumed period of operation. Presence of water in the subgrade can be one of the main factors affecting the structural capacity of pavement and can result in cracking of the bituminous layers, even after a very short period of trafficking. Reconstruction of one of regional roads in Poland has been chosen to serve as an example of inappropriate approach to the problem of the presence of water in the road structure. The project included construction of new layers of pavement and increasing the design life of the whole pavement structure to 4.06 million ESAL of 100 kN (as per the Standard Catalogue of Typical Flexible and Semi-rigid Road Pavement Structures, issue of 1997). After a relatively short period of trafficking (3-5 years) localised alligator cracking appeared on the surface along with structural deformations. The pavement condition assessment including FWD tests was carried out to reveal excessive deflections (over 500  $\mu\text{m}$ ) which classify the road for renewal. The analysis of data showed that the main cause of distress was softening of the subgrade caused by an ingress of precipitation water under the pavement layers through the roadway and shoulder edges. The deficiencies of the performed reconstruction occurred both in the roadway (including small step-outs in the cement-treated layer) and partly in the shoulders where the existing soil was in places replaced with impervious material, with the existing (cohesive) material left in place on a major part of the overall length.

## 1. Introduction

Pavement renewal or alteration works, when well performed, shall ensure the desired properties of the road during the assumed period of operation. Planning of such works should be preceded by comprehensive investigation of the existing condition of pavement, including the hydrogeological conditions of the soil subgrade. A well designed the road drainage system is also very important. Presence of water in the subgrade can be one of the main factors affecting its structural capacity and can result in fatigue cracking of the bituminous layers, even after a very short period of trafficking. The activities related to protecting the pavement from water must not be limited to dealing with ground water and attention must also be paid to storm water infiltrating under the pavement layers. Storm water should be evacuated, as soon as possible, beyond the area of the most severe traffic impact through open or closed (subsurface) drainage system. Quality of works and appropriate longitudinal profile of the pavement layers and subgrade are among the main factors ensuring efficient drainage and correct behaviour of the whole road structure.

Typical pavements are protected from infiltration of storm water by an impervious surface layer. This layer must have appropriate longitudinal and transverse slopes for efficient draining of water to



open ditches or to a closed drainage system. In open drainage systems particular attention must be paid to pervious dirt shoulder which may hinder the flow of water in places where it overtops the roadway edge elevation. As a result water may penetrate into the pavement structure. This can be particularly dangerous if water cannot drain towards open ditches through dirt shoulders made of cohesive materials and there is no proper drainage or separation layer in place.

## 2. Case Study – Current Situation

Due to a poor condition of the road and increasing level of traffic to be handled (including a large percentage share of HGV's) the road operator decided to undertake reconstruction of a 3.5 km long section of the road. The reconstructed section would be a single carriageway road with two 3.5 m wide traffic lanes and 0.70-1.2 m wide shoulders (varying). Subsurface conditions were investigated and ground water was not encountered (to 4 m depth below the bottom of pavement) while the subgrade soil was rated as most frost-susceptible (G class, clay). On this basis, taking into account the vertical alignment of the road the subgrade was classified in G4 strength group ( $E_2 \geq 25$  MPa) according to the Polish subgrade classification system. This rating was adopted in the design of the new pavement:

- Wearing course SMA 11 PMB 45/80-55 - 4 cm,
- Binder course AC 16 W 35/50 - 8 cm,
- Base course AC 22 P 35/50 - 10 cm,
- Base course Crushed stone 0/31,5 mm - 20 cm,
- Stabilized course  $R_m = 2,5$  MPa - 25 cm.

The design included strengthening of a 50-70 cm wide strip of shoulder with 15 cm thick layer of recycled asphalt pavement (RAP).

The pavement structure satisfies the frost-resistance requirement ( $H_{des} = 67$  cm  $>$   $H_{req} = 60$  cm).

The pavement structure has fatigue life of 4.06 million ESAL of 100 kN (calculated with the Asphalt Institute method [1]), i.e. is designed for KR4 traffic loading according to the Polish classification system. The reconstructed road was designed to ensure the properties of pavement at the required levels in the 20-year period of operation.

Taking into account the new issue of the Typical Flexible and Semi-rigid Pavement Design Catalogue [2] the fatigue life of pavement was calculated using the method of AASHTO 2004 [3]. Assuming the value of  $FC_{bottom}$  at 10% (for bottom-up fatigue cracking) fatigue life of 8.2 million ESAL of 100 kN was obtained, meeting the requirement for KR5 traffic loading. The governing criterion was fatigue cracking of the asphalt layers.

According to the construction program the works were to be carried out in spring and in summer. The scope of work included removal of existing layers, grading and compacting of the road subgrade, placing of the cement-treated soil layer ( $R_m = 2.5$  MPa) and finally placing the remaining layers of pavement. The soil removed from shoulders was to be reused subject to meeting the permeability requirement. However, the design did not specify the required properties of soil (neither grading or permeability). The pavement configuration showing connection with the dirt shoulder is presented in Fig. 1.

Fatigue cracks started to appear locally after 3-4 years of trafficking along with structural deformations (Fig. 2). The distress was most severe at low spots of the road (e.g., within concave vertical curves).

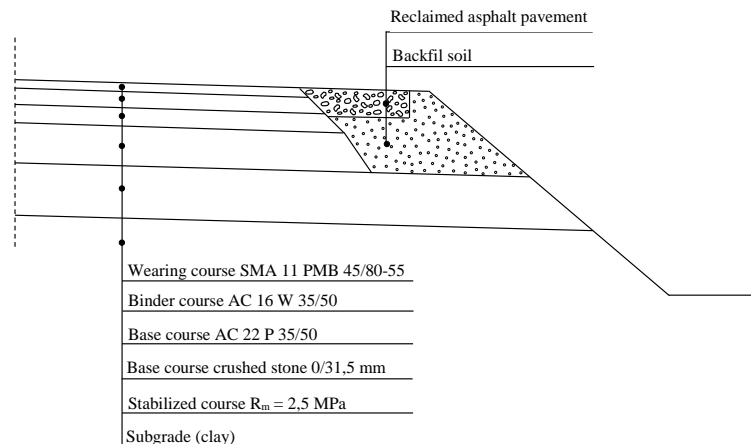


**Figure 1.** Layers of pavement reconstructed on voivodeship road.



**Figure 2.** Fatigue cracking and rutting after 3-4 years of open road into service.

### 3. Field and Laboratory Testing

A detailed field investigation was indispensable for correct determination of the causes of pavement distress. Non-destructive tests were performed in the first stage, including FWD tests to determine the structural capacity of the pavement and GPR tests to determine the thicknesses of the pavement layers. This stage of testing was commissioned by the road administrator. The tests were carried out in the first days of September in partly cloudy weather with no heavy rainfall and at ambient temperatures of 10-20°C. In the second stage (at the end of September) cores were cut from the pavement for more accurate thickness determinations and for testing the physical and strength properties of the pavement layers. Additionally, samples were taken from the shoulder.

Deflection tests were carried out early in the morning (for safety reasons) in the right wheel path. The test load of 50 kN ( $\pm 0.5$  kN) was applied at 25 m intervals. The temperature of the bituminous layers was adopted at 13-14°C. The deflections were measured with an array of geophones deployed at the plate centre and at pre-determined offsets of 200, 300, 450, 600, 900, 1200, 1500 and 1800 mm. The analysed parameters were the maximum deflections at the plate centre and surface curvature index SCI300. The maximum deflections at the plate centre on the slow lane are presented in Fig. 3. Similar results were obtained in the fast lane.

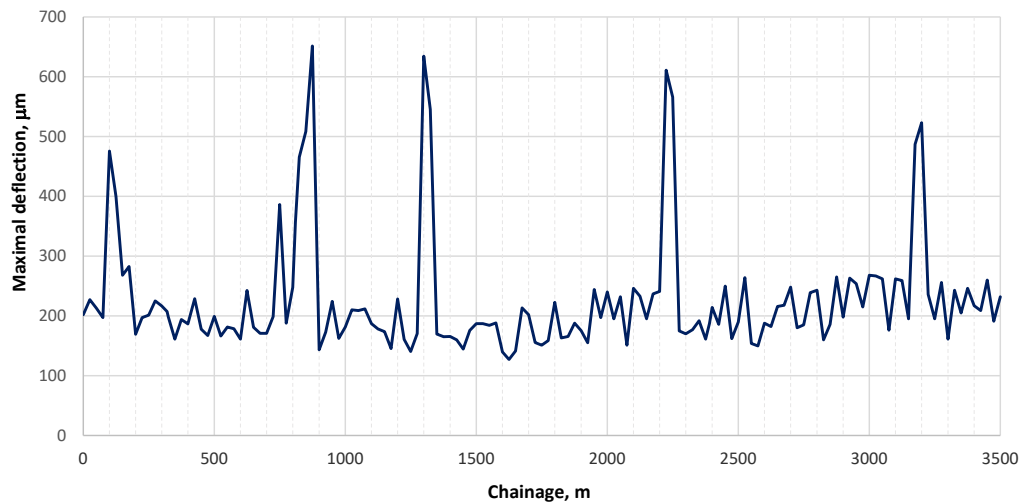


**Figure 3.** Maximal deflection from FWD test (nearest wheel, nearest line).

The maximum deflections at the plate centre can be classified in two groups. The first group includes results falling in the range from 125 to 270  $\mu\text{m}$  making up over 90% of all the results. The second group includes results obtained at twelve test points. There the deflections exceeded 350  $\mu\text{m}$ . This grouping of results was also relevant for the deflection bowl shapes. This concerns primarily much greater increase of deflection with the decreasing distance to plate centre recorded at these twelve test points where high values of maximum deflections were recorded. Fig. 4 presents the character of deformation obtained through deflection measurements on the respective geophones for the above-mentioned two groups of results.

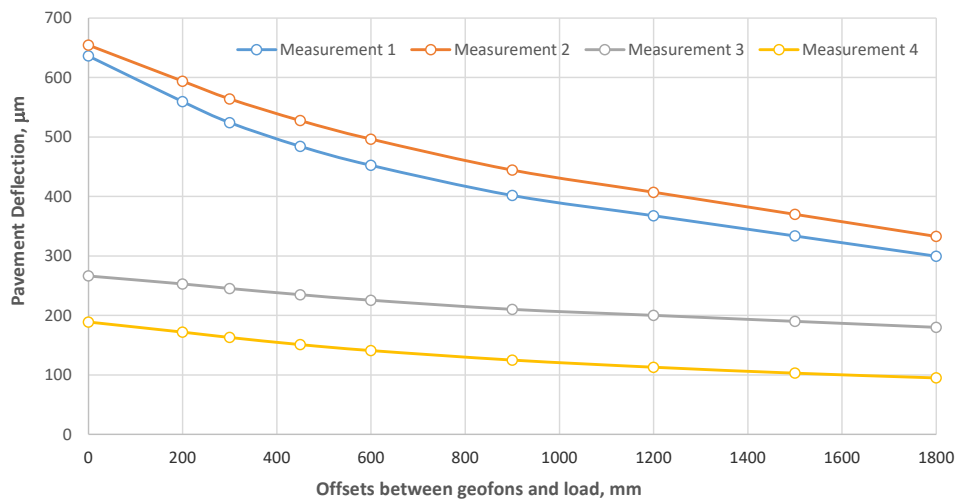


**Figure 4.** Pavement deflection in every geophone from FWD test (test 1 and 2 – places where are large maximal deflection, place 3 and 4 – places where are small maximal deflection).

In addition to determining the thicknesses of pavement layers the GPR system can also be used to detect changes or failures of the pavement structure, loss of bonding between pavement layers or excessive moisture content in the soil subgrade or base layers. The measurements were carried out with two antenna systems operating at different frequencies, namely 2.2 GHz and 1.0 GHz. The two antenna systems had different penetration depths: ca. 45 cm and ca. 90 cm. The results of thickness measurements on the both lanes are presented in Table 1.

Additionally, the layer thicknesses measured in the slow lane in relation to the road chainage are presented graphically in Fig. 5. The analysis of GPR results did not reveal any loss of bonding between the bituminous layers or excessive moisture content in the lower layers of the pavement structure (soil subgrade, cement-treated soil or crushed aggregate base).

**Table 1.** Layer thickness from ground-penetrating radar (GPR).

Statistical parameters	Asphalt layers		Base course Crushed stone		Stabilized course	
	Right lane	left Lane	Right lane	Left lane	Right lane	Left lane
Average [cm]	21.2	21.5	20.6	19.7	22.1	22.3
Standard deviation [cm]	2.5	2.2	2.8	2.7	3.6	3.2
Maximum value [cm]	25.5	24.3	25.6	24.7	28.5	28.2
Minimum value [cm]	17.0	17.3	16.0	16.7	16.8	17.3
Quantile 75% [cm]	19.1	18.9	18.2	18.4	19.7	19.4
Quantile 85% [cm]	18.2	18.4	17.2	17.7	18.4	18.5
Quantile 95% [cm]	17.4	17.7	16.3	16.6	17.4	17.3

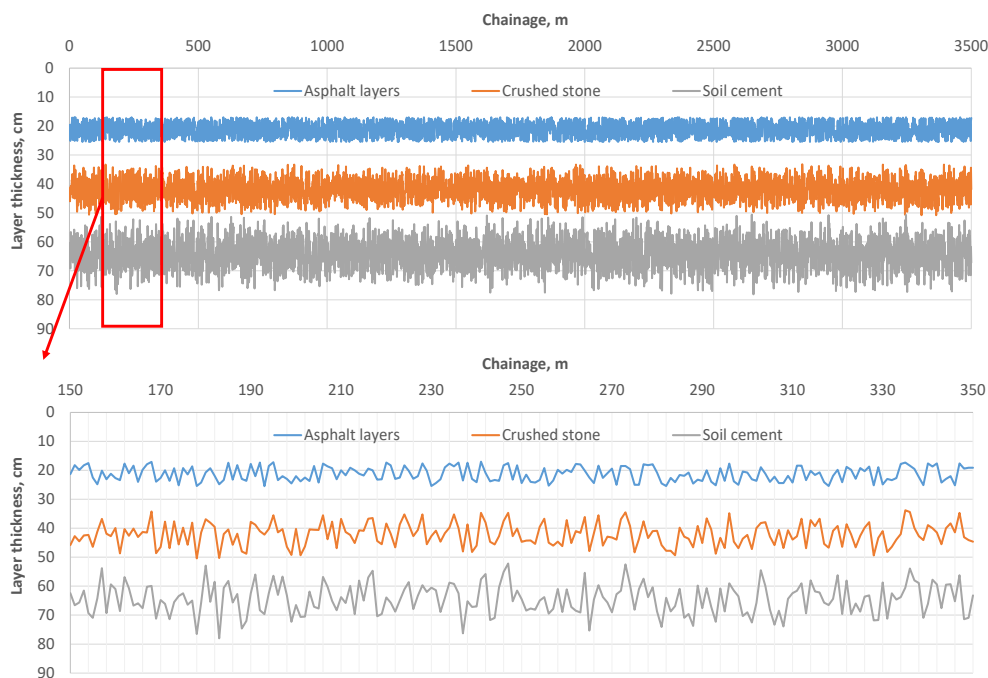


**Figure 5.** Layer thickness of pavement on nearest traffic line from ground radar test.

The next steps of investigation were defined by the review of FWD and GPR data. Particular attention was given to areas with insufficient structural capacity. The type of distress included both fatigue cracking and structural deformations. Samples of the respective layers were taken by cutting cores from the pavement on these sections. The coring locations were in places of maximum deflections (5 No.) and additionally at two points with small deflections for comparison. The scope of tests included determination of different parameters of the pavement layers, including their thicknesses, stiffness moduli determined with the indirect tensile test on cylindrical specimens (IT-CY), compressive strength of the cement-treated soil layer and CBR ratios of crushed aggregate base and of the subgrade soil. In test points 1-5 cores were cut in the cracked areas and their vicinity (at ca. 3-10 m distance). The samples taken from uncracked areas (bituminous mixtures and cement-treated soil designated “\*\*”) had undisturbed structure which enabled determination of the stiffness modulus

of the bituminous base course by the indirect tensile tests (IT-CY), determination of the relative compaction of this layer and determination of the compressive strength of the cement-treated soil layer. In areas of apparent cracks samples were taken from all the pavement layers and cracks were found both in the asphalt layers and in the cement-treated soil layer. This definitely confirms that cracks were initiated at the bottom of the pavement structure, i.e. in the cement-treated soil and in the bituminous road base layers. The test results are presented in Table 2.

**Table 2.** Parameters of pavement layers based on core drilling.

Parameter	Sample						
	1	2	3	4	5	6*	7*
Chainage, m	100	875	1300	2225	3200	925	2600
Asphalt layers thickness, cm	21.7 / 21.2**	23.5 / 22.8**	22.4 / 23.1**	21.1 / 21.7**	22.6 / 22.3**	19.6	21.1
Compaction factor (AC 22 P), %	- / 97.6**	- / 99.4**	- / 98.7**	- / 100.3**	- / 98.5**	99.2	98.3
Voids in total mix (AC 22 P), %	- / 6.9**	- / 5.3**	- / 6.2**	- / 4.8**	- / 6.1**	5.5	6.4
Crushed stone layer thickness, cm	- / 23.4**	- / 17.2**	- / 22.4**	- / 19.2**	- / 17.1**	23.2	19.6
Stabilized course layer thickness, cm	- / 24.3**	- / 24.0**	- / 23.6**	- / 23.6**	- / 23.8**	21.8	23.6
Stiffness module IT-CY, 20°C, MPa	- / 7654**	- / 7023**	- / 6578**	- / 6487**	- / 7787**	6203	7436
Compressive strength of stabilized course, MPa	- / 3.26**	- / 3.51**	- / 2.96**	- / 4.12**	- / 2.67**	3.75	4.06
California bearing ratio of crushed stone, %	124	141	138	126	154	131	129
California bearing ratio of subgrade(optimum moisture), %	14	9	13	16	11	12	17
California bearing ratio of subgrade (4-day soaked), %	5	2	3	3	4	2	3

\* place where pavement wasn't destroyed, \*\* place next to where pavement was destroyed (3 - 10 m)

The structure of the cement-treated soil in the area affected by surface cracking was disturbed, specifically it was partly mixed with both crushed aggregate and with subgrade soil.

Soil samples taken from the subgrade featured a relatively high bearing capacity when tested at optimum moisture content (70 to 108 MPa elastic modulus according to Powell). With increasing moisture content the bearing capacity decreased considerably and so did the value of the elastic modulus (25 to 50 MPa). This could be one of the causes of the observed structural failures.

The soil in the shoulder area was found to be highly diverse. It included both loose material (medium and coarse sand) and cohesive material (clay, silty clay, pre-Quaternary clay, loamy sand), the latter type of material being in majority.

#### 4. Analysis of the Test Results

One of the main performance characteristics which is used to rate the condition of pavement is the elastic deflection. It can be determined by FWD measurements. The parameters measured during this tests include the maximum deflection at the plate centre, which is converted to normalised deflection value (according to [4, 5]) and used for determining uniform sections (for example with the cumulative sum chart). The equivalent deflections are then calculated for these uniform sections. The second parameter is the surface curvature index SCI300 calculated as a difference between the centre deflection and the deflection measured at 300 mm distance from the plate centre. These two parameters are used to determine the so-called decision level by assigning condition rating to the pavement [4, 5].

Fig. 6 presents the normalised deflection values (obtained by converting the results to standard conditions of 50 kN weight and 30 cm plate diameter and 20°C temperature, taking into account the season of the year and the road base material) as cumulative sums.

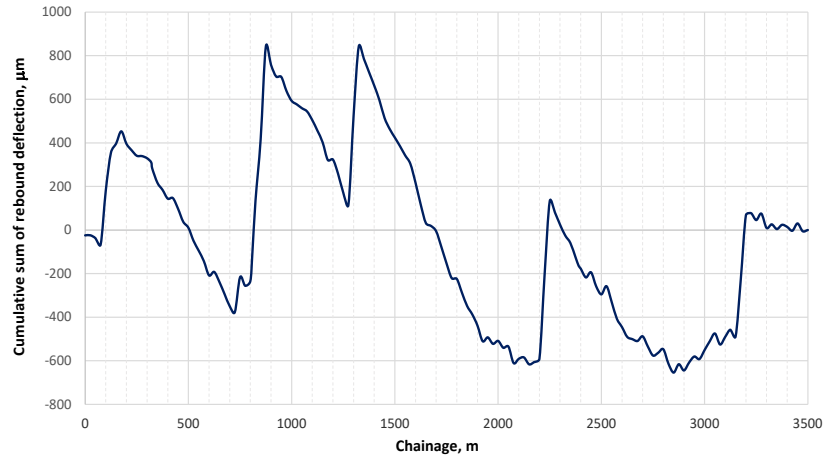


**Figure 6.** Cumulative sum of rebound deflection on voivodeship road.

It clearly transpires from Fig. 6 that higher values were obtained in isolated spaces influencing the shape of the curve and the number of uniform sections. In order to obtain a better illustration of the effect of places with deflections exceeding the maximum allowed value basic static calculations were conducted for the whole analysed section (before adjustment) and for the section without areas with higher deflections (after adjustment) for both lanes (Table 3).

**Table 3.** Statistics of deflection measurements on left and right lane.

Statistical parameters	Right lane		Left lane	
	Before correction	After correction	Before correction	After correction
Average [ $\mu\text{m}$ ]	303.8	266.9	295.4	254.5
Standard deviation, $D_U$ [ $\mu\text{m}$ ]	133.8	48.4	138.7	46.2
Maximum value [ $\mu\text{m}$ ]	875.3	380.1	891.5	376.9
Minimum value [ $\mu\text{m}$ ]	170.8	170.8	175.3	167.8
Standardized deflection (deflection index), $U$ [ $\mu\text{m}$ ]	437.6	315.3	434.1	300.7
Quantile 85% [ $\mu\text{m}$ ]	349.4	326.6	334.3	311.8
Quantile 95% [ $\mu\text{m}$ ]	654.5	352.9	626.9	334.5

According to the results presented in Table 3 the differences between the average measured deflections before and after adjustment fall in the range of 36-40  $\mu\text{m}$ . Much greater differences are obtained for the typical deflections, namely ca. 120-130  $\mu\text{m}$ . This is attributed to high statistical variability indicated by the value of standard deviation. The equivalent deflections obtained after omitting weak spots correspond to the values specified for the KR4 traffic loading in the DSN pavement rating system used in Poland (except for a small exceeding in the slow lane). When the whole section is considered the equivalent deflection is close to the value critical for KR4 traffic loading (on both travel lanes) and immediate renewal is required.

The equivalent value of the curvature index SCI300 which is one of the parameters for rating the bearing capacity of pavements is calculated as the sum of the average standard deviation of SCI300 values for the whole section (before adjustment), for the section without higher deflection areas and for high deflection areas. These values, together with additional statistical parameters for SCI300 curvature index, are presented in Table 4.

**Table 4.** Statistical parameters, Surface Curvature Index SCI300.

Statistical parameters	Right lane			Left lane		
	before correction	after correction	high deflection	before correction	after correction	high deflection
Average [ $\mu\text{m}$ ]	63.3	43.5	261.9	65.7	41.8	252.1
Standard deviation, $D_U$ [ $\mu\text{m}$ ]	66.0	11.2	55.5	62.1	10.4	53.2
Maximum value [ $\mu\text{m}$ ]	366.6	78.4	366.6	339.2	79.2	339.2
Minimum value [ $\mu\text{m}$ ]	28.1	28.1	197.4	32.2	32.2	169.8
Surface Curvature Index SCI [ $\mu\text{m}$ ]	129.3	54.6	317.4	127.8	52.2	305.3
Quantile 85% [ $\mu\text{m}$ ]	66.5	54.4	296.7	67.2	49.5	284.2
Quantile 95% [ $\mu\text{m}$ ]	233.3	69.3	343.3	206.8	64.3	326.9

Considering the equivalent curvature index values for the whole section (including higher deflection areas) the road obtains C rating for KR4 traffic loading (at the boundary of D rating). Note that for KR5 traffic loading the condition rating would be D and the road would require renewal (according to [5]). When the areas with increased deflections are left out the road gets B rating for both KR4 and KR5 traffic loading. In higher deflection areas the values of SCI were very high, considerably exceeding the limit of D rating irrespective of the traffic loading. This clearly indicates damage to bituminous layers, resulting in distribution of stresses on a smaller area of soil subgrade.

For selected locations (two high deflection spots marked B and two low deflection spots marked L) the resilient moduli were back-calculated for the respective layers of pavement. For the crushed aggregate sub-base a constant value of the resilient modulus was adopted at 400 MPa. The thicknesses of the pavement layers were determined on the basis of GPR data. The thickness of the soil subgrade layer was taken at 5.9 m. The calculation results are presented in Table 5.

**Table 5.** Stiffness module from „backcalculation”.

Layer	B1		B2		L1		L2	
	$h$ , mm	$S$ , MPa						
	204	2175	216	2841.4	224	15336.4	221	9431.0
Base course Crushed stone	190	400*	200	400*	236	400*	229	400*
Stabilized course	225	567.1	236	454.9	257	7097.2	240	6237.8
Subgrade	5000	45.8	5000	37.8	5000	101.8	5000	109.9

\* – constant value for calculations,  $h$  – layers thickness,  $S$  – Stiffness module (modulus of elasticity)

The calculated values show much smaller resilient moduli of the bituminous and cement-treated soil layers in high deflection areas, as compared to areas where smaller deflections were obtained in measurements. This is in agreement with the structural damage of these layers due to cracking. Different resilient moduli were also obtained for the subgrade. This could be attributed to a higher moisture content affecting its bearing capacity.

Insufficient thickness of pavement layer(s) or their mechanical properties (compaction, strength, etc.) were excluded as the causes of pavement distress on the basis of GPR data and determinations on undisturbed samples taken at the damaged sites. During the site visit it was established that the defective areas are located at low spots along the road. Consequently, longitudinal profile measurements were carried out. The vertical alignment of the road, related to the maximum deflections measured with FWD is presented in Fig. 7.

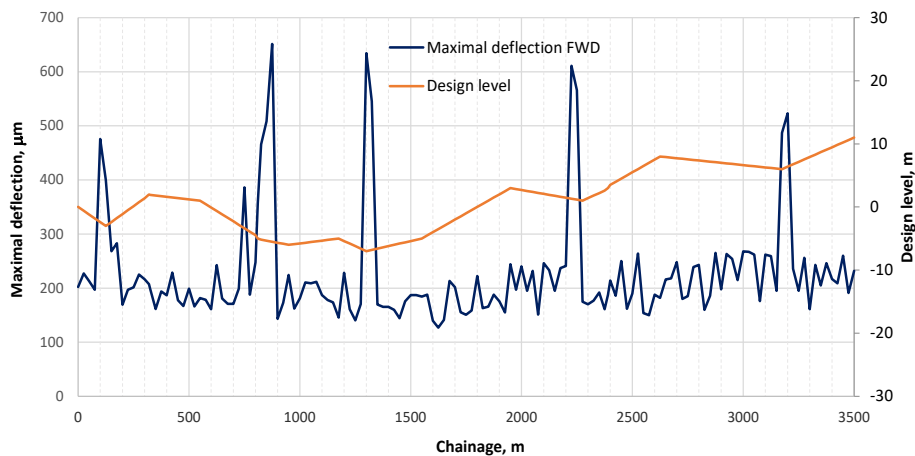


**Figure 7.** Road vertical alignment with maximal deflection.

From the analysis of results presented in Fig. 7 it can be seen that the greatest deflections coincide with concave vertical curves. Storm water could pond there and penetrate under the structure through the edge of dirt shoulder. This affected the bearing capacity of subgrade and, subsequently, also of the pavement courses, in particular the layers of increased stiffness, i.e. cement-treated and bituminous.

At the dips of the road profile storm water penetrates under the pavement structure when it cannot drain into open ditches. This suggests that efficient drainage of water outside the roadway prism was not ensured during the works. In order to verify this, test pits were dug at pre-determined locations at the road edge. It was found out that the cross section and the layer locations vary and conform to the design only in places (Fig. 1), deviating from it on a major part of the section, in particular where shoulder extends in width - see Fig. 8.

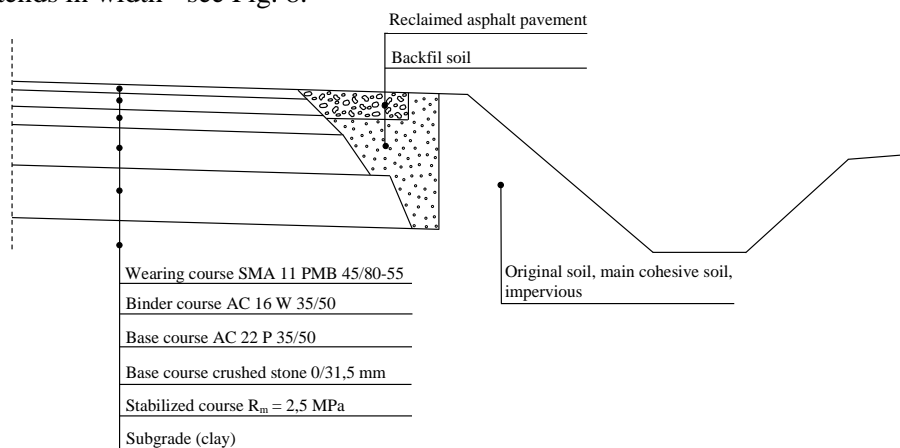


**Figure 8.** Cross section of road with marginal strip.

## 5. Summing up

The analysis of the test and measurement data and findings from condition assessment indicate that the causes of distress should not be attributed to insufficient thicknesses of pavement courses or to the values of their performance parameters. This has been confirmed by comparing the data obtained at the places of distress, in their immediate vicinity and in areas where no apparent damages were found.

Therefore, with a high degree of probability we can attribute the cause of pavement distress to bearing failure of the subgrade soil which was caused by storm water penetration. Plastic yielding of soil in the subgrade caused structural failure of the cement-treated soil layer and, subsequently, also of the bituminous layers. This is confirmed by the bearing capacity data obtained in FWD test and by the condition of the pavement courses.

It clearly transpires from Fig. 8 that accumulation of storm water under the pavement and plastic yielding of subgrade soil was caused by reduced width of the cement-treated soil layer and replacement of the native soil in the shoulder with loose material (permeable and non-swelling). The native soil which was left undisturbed in the shoulder area has varying composition in which cohesive, swelling and impervious materials prevailed. An additional factor hindering the flow of storm water were higher places in shoulder area (beyond the RAP strip) created by growth of vegetation.

The recommended treatments include immediate repair of the affected areas, replacement of the shoulder material and widening of the cement-treated soil layer to the whole width of the road prism.

### References

- [1] Katalog Typowych Konstrukcji Nawierzchni Podatnych i Półsztywnych. IBDiM, GDDKiA Warszawa 1997
- [2] Katalog Typowych Konstrukcji nawierzchni Podatnych i Półsztywnych. Załącznik do zarządzenia nr 31 GDDKiA, Politechnika Gdańska, 2014
- [3] Judycki J., Jaskuła P., Pszczoła M. i inni: Analizy i projektowanie konstrukcji nawierzchni podatnych i półsztywnych. WKiŁ, Warszawa 2014
- [4] System oceny stanu nawierzchni SOSN. Wytyczne stosowania. GDDKiA. Załącznik do Zarządzenia Nr 5 z dnia 01.02.2010
- [5] Diagnostyka stanu nawierzchni i jej elementów. Wytyczne stosowania. GDDKiA. Załącznik do zarządzenia Nr 34 GDDKiA z dnia 30.04.2015